

ECRH for W7-X: Transmission losses of high-power 140 GHz wave beams

V. Erckmann¹, W. Kasperek², G. Gantenbein³, F. Hollmann¹, L. Jonitz¹, F. Noke¹, F. Purps¹,
M. Weissgerber¹, and the W7-X ECRH- teams at IPP Greifswald¹,
FZK Karlsruhe² and IPF Stuttgart³

*1 Max Planck Institut für Plasmaphysik, EURATOM Association,
Teilinstitut Greifswald, D-17491 Greifswald, Germany*

2 Institut für Plasmaforschung, Universität Stuttgart, D-70569 Stuttgart, Germany

*3 Forschungszentrum Karlsruhe, Association EURATOM-FZK, IHM,
Hermann-von-Helmholtz-Platz 1, D-76344 Eggenstein-Leopoldshafen, Germany,*

Information on the corresponding author:

Volker Erckmann

Max Planck Institut für Plasmaphysik,

Wendelsteinstrasse 1, D-17491 Greifswald, Germany

e-mail: volker.erckmann@ipp.mpg.de

Phone: +49-3834-88-2450 Fax: +49-3834-88-2459

Pages: 23 (incl. ref., tables, Figures and Fig. captions)

Tables: 4

Figures: 5 (Fig 1,2,3 should be published in colors)

Abstract:

Electron Cyclotron Resonance Heating (ECRH) is the main heating system for W7-X. A 10 MW ECRH plant with cw-capability is under construction to support the W7-X operation, which aims at demonstrating the steady state capability of stellarators at reactor relevant plasma parameters. The ECRH system consists of 10 RF-modules with 1 MW power each at 140 GHz. The RF-beams of the individual gyrotrons are transmitted in common to the W7-X torus via open multi-beam mirror lines. The losses of individual components of the transmission system were measured with both, low- and high-power methods. Integrated full power, cw measurements of the long-distance transmission losses are reported and compared to theoretical design estimates.

PACS: 52.50.-b, 52.35.Hr, 52.55.Hc, 52.70.Gw, 41.20.Jb, 84.40.-x, 84.40.Az

I. INTRODUCTION

Electron Cyclotron Resonance Heating (ECRH) is the main heating system for steady state operation of the W7-X Stellarator, which is the next step in the stellarator approach towards magnetic fusion power plants. In contrast to Tokamaks, Stellarators have inherent steady state operation capability because the confining magnetic field configuration is generated by external coils only. W7-X is equipped with a superconducting coil system, a continuously operating ECR-heating system and an actively pumped divertor for stationary particle and energy control. An ECR-heating power of 10 MW at 140 GHz is required to achieve fusion relevant plasma parameters in W7-X at the nominal magnetic field of 2.5 T [1]. The physics demands for different operating scenarios such as 2nd harmonic X and O-mode, 3rd harmonic X- mode and O-X-B- mode conversion heating [2,3,4] can only be met with a very flexible transmission system, which allows for almost arbitrary mode selection and transmission. The gyrotron radiation is linearly polarized and the transmission system must be capable of converting the gyrotron radiation to all polarizations from linear (perpendicular launch) to circular polarization (oblique launch) and transmitting them with low losses. As the W7-X ECRH can also operate at 103.6 GHz with reduced power, broadband transmission is also mandatory. An optical transmission system was developed for W7-X, which is the most simple, reliable and cost effective solution [5,6]. Here, the millimeter waves are transmitted as a Gaussian beam by iterative transformation with metallic mirrors. Main advantages of this technology are the low (ohmic and diffractive) losses, the high power capability due to relatively low field strength and the inherent mode filtering as high-order modes are diffracted out of the system.

For each gyrotron, a beam conditioning optics consisting of five single-beam mirrors is used. Two of these mirrors form the matching optics unit (MOU) and convert the gyrotron output to a Gaussian beam with the correct beam parameters. The following two mirrors have a sinusoidal surface corrugation [7] to set the polarization needed for optimum absorption of the radiation in the plasma [8], a fifth mirror finally directs the beam towards the beam combining optics.

The long-distance transmission of the RF-power to the ports of the W7-X torus (typically 60 m) is performed by two open multi-beam waveguide (MBWG) lines operating at normal pressure, each of them transmitting (and handling) 5 (+2) individual RF-beams (7 MW). The power handling capability has inherently a large safety margin of a factor of 2-3 due to the low power density on the mirror surfaces. A later power upgrade of the ECRH-system by replacing the 1 MW gyrotrons by more powerful ones (if such gyrotrons become available) is possible without any modification of the transmission line. An underground concrete duct houses the individual components of the transmission system as sketched in Fig.1. The gyrotrons are installed behind the wall of the duct and radiate their power laterally through small holes in the duct-walls. The concrete walls are an efficient absorber of stray radiation from the open lines thus satisfying the safety requirements on microwave shielding. All mirrors in the beam duct are remotely controlled.

The individual components of the transmission line are briefly described in Sec. II and the losses induced by the most relevant components are discussed. Integrated full power, cw experiments with long-distance transmission are reported in Sec. III and the measured losses are compared to low power measurements and theoretical modelling. Finally, in Sec. IV we summarize the high- and low-power transmission results and draw some conclusions.

II. THE TRANSMISSION SYSTEM: CHARACTERISTICS AND LOSSES

The overall transmission efficiency is determined by several loss-channels. In general, the rf-emission of a gyrotron has a directed beam-component and a stray radiation component. The latter is originating from the imperfect gyrotron mode converter and internal mirror assembly. The stray radiation (typically less than 5 %, for the TED Gyrotron SNo.1 about 3 % [9]) is emitted through the window under arbitrary angles and has to be dumped by water-cooled absorbers and the concrete walls of the beam duct, see Sec. II.A. The directed beam carries typically more than 95 % of the total rf-power and is, in general, a mode mixture of the desired Gaussian fundamental mode with some spurious high order free space modes. The conversion to a pure fundamental Gaussian beam with the correct beam parameters is performed by the two-mirror MOU. The losses depend on the gyrotron beam-quality and are somewhat different for each gyrotron. The worst-case losses are 5 % for the W7-X gyrotrons and the related MOU [9]. As this is a significant loss channel, there is still some benefit in improving the gyrotron output beam quality further. Besides ohmic dissipation in the mirrors and diffraction loss due to mode conversion and mirror surface deformation, further sources of loss are beam truncation of the reflectors and windows, misalignment and atmospheric absorption. The estimated worst case contributions are listed in Table I. One can see, that a total transmission efficiency of ≥ 85 % is expected. The ‘Diffraction and beam truncation’ losses of ≤ 2 % in Table I are calculated from nominal truncation and the resulting diffraction of 0.067 % per mirror (about 1 % in total) plus additional diffraction losses of about 1 % due to imperfect mirror surfaces, assuming that the mirrors are machined according to the specifications. These losses are reduced in case, that the mirror surfaces are machined with higher quality. The figure for ‘misalignment losses’ in Table I is based on reasonable assumptions, but is probably somewhat pessimistic. As will be shown in Sec. III, the measured overall losses can only be explained with a negligible (within the error bars) contribution of misalignment losses.

The ECRH system for W7-X will finally comprise more than 160 water-cooled mirrors for beam matching and polarization adjustment, transmission, switching of beams, and for the front steering launchers. Due to the complexity of the system and to test its performance and stability, a full-scale prototype has been built, which consists of a lens horn with beam parameters similar to the W7-X gyrotrons, a 5-mirror matching assembly and one MBWG system. The total transmission efficiency of the prototype system including the diffraction due to imperfect surfaces, ohmic loss, typical misalignment, and atmospheric absorption was checked by calorimetric methods and yielded $90\pm 2\%$ [10]. This is in good agreement with the theoretical value for the prototype system, which is 92 %, if only the reflection loss of 18 Aluminium surfaces (5.3%), the diffraction and truncation on the mirrors (1.6%) and the atmospheric absorption (1.5%) is taken into account.

II.A Stray Radiation Losses

Due to the imperfect mode conversion from a high-order cavity mode (e.g. TE 28.8 for the TED-Gyrotron) to a fundamental Gaussian free space mode TEM₀₀ inside the gyrotron [11,12], some amount of non-directed radiation is emitted through the gyrotron window under steep angles and must be absorbed. The microwave beams are therefore transmitted through a stainless-steel shielding pipe of about 1.2 m length with an absorbing layer of water cooled Teflon pipes wound onto the inner surface. The front end of this beam tube is seen from Fig. 2. As the Teflon pipe is transparent for microwaves, the stray radiation is absorbed directly by the water flowing in the pipes. An additional stray radiation absorber is installed behind mirror 1 ('japanese umbrella', see Fig. 2), which handles the stray radiation with grazing incidence to the beam tube walls with imperfect absorption, as well as spill over losses and side lobes of the directed gyrotron beam. The losses can be easily measured calorimetrically in such a system and are listed in Table II. The data were measured under

high-power, stationary conditions (typical 0.6 - 0.7 MW, 5-7 min operation).

For the particular case of a slightly damaged gyrotron with a deformed internal mode converter and a correspondingly bad rf-beam with pronounced astigmatism and side lobes, increased losses as high as 3.7 % were measured in the beam tube, which may be due to both, enhanced stray radiation inside the gyrotron and side lobes of the directed output beam. It should be noted, that the measured stray radiation of 4.6 % in the beam tube and Japanese umbrella cannot be reconverted and is wasted power in any case. This power will be accounted for in calculating the overall gyrotron efficiency, but not for the determination of the external transmission efficiency.

The ‘teflon pipe’ based absorber technology is very simple and versatile and was applied in different absorbing components of the transmission system such as the short-pulse calorimetric load, the preload for the cw- dummy load, and the large scale stray radiation absorber in the MBWG-section, the latter is seen in Fig. 3.

II.B Ohmic losses from copper mirrors and polarizers

For 140 GHz radiation reflected from an ideal copper surface at perpendicular incidence, the theoretical absorption is 0.1035 % [13]. To get data for the real ohmic loss of different copper surfaces (plane; shallow diagnostic gratings; polarizing grooves) with typical machining quality, a resonator technique was used c.f. [14]. The measured losses were found to be about a factor of 1.2 ...1.5 above the theoretical value for plane and shallow grating surfaces. For polarizing surfaces with corrugation, the ohmic losses are strongly dependent on the orientation of the electric rf-field with respect to the grooves. A linear polarized wave with the electric field vector parallel to the grooves (TE-polarization) suffers only from a moderate increase of the loss by a factor of 1.61.85 compared to ideal plane surface as measured in the low power set-up. For the electric field perpendicular to the grooves (TM polarization) the loss is

significantly higher as the wave can penetrate into the grooves. The first of the two polarizers, which are required to set an arbitrary wave polarization, is an elliptical polarizer (P1) with a groove period of 1.28 mm and a groove depth of 0.56 mm, respectively. P1 shifts the polarization between the TE and the TM wave by 90° , thus any ellipticity of the reflected radiation can be set by proper rotation of the grooved mirror around its axis of symmetry. The second polarizer (P2, groove period = 1.28 mm, groove depth = 0.78 mm) has a corrugation for a 180° phase shift to turn the axis of the polarization ellipse to the appropriate orientation.

For the elliptical polarizer P1 the losses measured by low power techniques are increased by a factor of 2.9, for the polarization rotator P2, an increase of a factor of 3.8 is found compared to an ideal plane surface.

We have measured the ohmic losses of P2 under high-power conditions calorimetrically using the mirror cooling circuit. The total incident beam power was measured with a calorimetric high-power cw-load. The beam power was adjusted to 0.59 MW with a pulse duration of 30 s, which is sufficient to achieve stationary conditions for the calorimetric measurements in both, the polarizer and the dummy load. The power incident on P2 is slightly higher (about 1 %), because of the additional transmission losses between the polarizer and the dummy load (3 mirrors, 1 polarizer). The results are shown in Fig. 4. In the first scan P1 was rotated from 0 deg to 45 deg, while keeping P2 fixed at 0 deg, i.e. the polarization incident on P2 changes from linear to circular, see Fig. 4 (top). The losses increase as expected from 0.14 % with a linearly polarized wave incident on P2 (E-vector parallel to the grooves) to 0.29 % for the circularly polarized wave. The high-power results are in very good agreement with the low power measurements. In a second scan we have kept P1 at 0 deg, i.e. a linearly polarized beam is incident on P2, and P2 was rotated from 0 deg (E-vector parallel to the grooves) to 90 deg (E-vector perpendicular to the grooves), see Fig. 4 (middle). The losses increase as expected from 0.14 % (E-vector parallel to the grooves) to 0.38 % (E-vector perpendicular to the grooves).

The normalized data are summarized in Table III, where the low- and high-power measurements are compared with parallel and perpendicular wave polarization, respectively, for selected reflection angles. For the W7-X transmission system, this results in a maximum loss for the polarizers of 3.8 kW per Megawatt incident beam power and a thermal peak loading of up to 75 W/cm² on the polarizer surface.

In a third scan we have varied the power incident on P2 from 0.4 to 0.76 MW for a setting with P1 at 45 °, generating circular polarization incident on P2, which was set to 20°. The expected linear dependence between incident and absorbed power in P2 for fixed P1 was confirmed within the error bars as seen from Fig.4 (bottom). The uncertainty in the polarizer calorimetry is about 70 Watt corresponding to 0.1 deg temperature difference in the calorimetric set-up.

III INTEGRATED LOSSES FOR LONG-DISTANCE TRANSMISSION

Tests of the entire transmission line can only be performed, once the W7-X construction is completed and access to the main torus hall is provided. We have therefore installed retro-reflectors SR in the underground beam duct in the image plane at half distance of the MBWG transmission line between mirrors M7 and M8. Long-distance transmission can then be simulated and tested by transmitting the high-power beams half way in forward direction and then back via the retro-reflectors to the dummy load. The arrangement of the different mirrors is seen from Fig.1, a photograph of both retro-reflectors and four symmetric MBWG-mirrors in the beam duct is seen in Fig. 3. The rf-beam passes through the 5-mirror array of the MOU, through the beam-combining optics unit M4, multi beam waveguide mirrors M5, M6, M7 towards the retro-reflector SR (two mirrors), backwards through M7, M6, M5 to M4 and back via SD and MD to the dummy load D. The incident power is measured while transmitting the reference beam through the 5-mirror array of the MOU, the beam-combining optics unit M4, and via MD towards the dummy load. The difference between both measurements then

accounts for altogether 10 reflections on the 2 x 3 MBWG-mirrors plus the 4 additional guiding mirrors over a total length of about 40 m for the selected beam. Note, that other beams have different propagation length depending on the gyrotron position. With the ohmic losses known for the different components as reported in Sec. II, the losses, which are introduced by diffraction and atmospheric damping, can be derived from integral measurements of the long-distance transmission. First high-power measurements are shown in Fig. 5, where the calorimetrically measured transmitted power is plotted vs. the incident power. As a guide for the eye, we have plotted the ‘no-loss’ line also. Total losses of about 3 % were measured, and are compared to the measured ohmic and calculated diffraction losses for the individual components in Table IV. The atmospheric damping was calculated using the measured humidity of the air in the beam duct. Very good agreement is found with calculations and previous low power measurements. This result confirms that the transmission line operates close to the theoretical loss-limit thus indicating the high quality of the quasi-optical concept for high-power, long-distance transmission.

IV SUMMARY AND CONCLUSIONS

The ECRH-system for W7-X is the most ambitious and largest cw-plant presently under test. The 10 MW, cw ECRH-power is transmitted via a quasi-optical multi-beam waveguide system operating at atmospheric pressure, which is a unique feature of this system. The quasi-optical transmission offers favorable characteristics such as broadband transmission and a high power handling margin. This allows operation of the system at two frequencies and with the option of a later power upgrade without modification of the transmission line. The most loaded components of the beam conditioning single beam section were tested and the losses were measured under high-power, cw conditions. Long-distance transmission through the multi-beam waveguide system was investigated. An excellent performance with low losses close to the theoretical losses was obtained under full power, cw conditions.

Acknowledgment

The authors wish to thank the technical staff at IPF, FZK and IPP for their excellent contributions in solving numerous technological problems during the R&D of the ECRH-transmission line components. We would like to thank all partners in the collaborating research laboratories for their stimulating discussions and active support.

References

- [1] V. ERCKMANN, H.J. HARTFUß, M. KICK, H. RENNER, et al.:
Proc. 17th IEEE/NPSS Symposium on Fusion Engineering, San Diego, USA (1997).
Ed. IEEE, Piscataway, NJ 1998, 40 – 48
- [2] V. ERCKMANN, P. BRAND, H. BRAUNE, G. DAMMERTZ, et al.:
Electron Cyclotron Heating for W7-X: Physics and Technology
Fusion Science and Technology, Vol. 52, No.2 (2007) pp. 291-312
- [3] M. ROME', V. ERCKMANN, U. GASPARINO, N. KARULIN :
Plasma Phys. Control. Fusion **40** (1998) 511-530
- [4] H. P. LAQUA, V. ERCKMANN, H.J. HARTFUß, H. LAQUA, W7-AS TEAM, AND
ECRH GROUP, *Phys. Rev. Lett.* **78**, 3467 (1997)
- [5] L. EMPACHER, W. FÖRSTER, G. GANTENBEIN, W. KASPAREK, et al.:
Conceptual Design of the 140 GHz/10 MW CW ECRH system for the Stellarator
W7-X, *Fusion Technology, Vol. 1 (1996) pp. 541-544*
- [6] L. EMPACHER AND W. KASPAREK:
Analysis of a multiple beam waveguide for free space transmission of microwaves
IEEE Trans. Antenna Propagation, Vol. AP-49 (2001) pp 483-493
- [7] KOPP, K.W., KASPAREK, W., HOLZHAUER, E.:
Microwave reflection properties of grooved metallic mirrors.
Int. J. Infrared and Millimeter Waves **13** (1992) 1619 – 1631
- [8] HEALD, M.A. and WHARTON, C.B.:
Plasma Diagnostic with Microwaves.
New York: J. Wiley and Sons 1965
- [9] M. THUMM, S. ALBERTI, A. ARNOLD, P. BRAND, et al.:
EU Megawatt-Class 140-GHz CW gyrotron.
IEEE Trans. Plasma Science, PS-35 (2007) pp 143 – 153.
- [10] W. KASPAREK, G. DAMMERTZ, V. ERCKMANN, G. GANTENBEIN, et al.:
The transmission system for ECRH on the Stellarator W7-X: Design issues and test of
prototype components.
Strong Microwaves in Plasmas, ed. A.G. Litvak, ISBN 5-8048-0039-6, Nizhny
Novgorod, Russia (2003) Vol. 1, 333 – 339.
- [11] G.G. DENISOV, A.N. KUFTIN, V.I. MALYGIN, N.P. VENEDIKTOV, D.V.
VINOGRADOV, AND V.E. ZAPEVALOV:
Int. J. Electronics, vol. 72, pp. 1079-1091, 1992.
- [12] S.N. VLASOV, L.I. ZAGRYADSKAYA, AND M.I. PETELIN:
Radio Eng. and Electron Physics, Vol. 20, (1975) pp. 14-17

- [13] GOLDSMITH, P.F.: Quasi-optical Systems. New York: IEEE Press, Chapman and Hall, Publishers, ISBN 0-7803-3439-6, 1998
- [14] KASPAREK, W.; FERNADEZ-CURTO, A.; HOLLMANN, F. AND WACKER, R.:
Measurement of ohmic loss of metallic reflectors at 140 GHz by a 3-mirror resonator technique,
Int. J. Infrared and Millimeter Waves **22** (2001) 1695-1707.

Tables

Loss channel	(Number of) elements	Loss
Gyrotron Mode transformation loss	Matching Optics Unit (2 mirrors)	$\leq 5\%$
Absorption on mirrors (av. over polarization)	14 plane + 2 grooved Cu surfaces	2.5 %
Diffraction and beam truncation	16 reflectors	$\leq 2\%$
Misalignment	Transmission line	$\leq 2\%$
Atmospheric absorption	60 m dried air / max.	0.8 % / 2%
Beam truncation, launcher	1 Window + 2 int. mirrors	3 %
TOTAL LOSS		$\leq 15\%$

Table I: Estimated contributions to the transmission loss.

Loss channel	Type	Loss
Beam tube	Gyrotron stray radiation	2.8 %
Japanese umbrella	High order directed, stray radiation	1.8 %
TOTAL LOSS		4.6 %

Table II: Stray radiation losses near the gyrotron.

Component	Calculated (ideal) losses (%)	Experiment Low power (%)	Experiment High power (%)
Mirror H-plane, $\alpha = 45^\circ$	0.0732	0.088	-
Polarizer P2, TE, E-plane, $\alpha = 10^\circ$		0.194	0.14
Polarizer P2, TM, E-plane, $\alpha = 10^\circ$		0.40	0.38

Table III: Comparison of the ohmic losses for a standard mirror and polarizer P2 with the linear polarization of the incident wave beam parallel (TE) and perpendicular (TM) with respect to the grooves. The angles of incidence α and the polarization plane is indicated.

Component	Ohmic losses (%)	Diffraction losses (%)	Total (%)
M5, M6, M7 (forward)	0.39	0.2	0.59
2 SR	0.26	0.1	0.36
M7, M6, M5 (backward)	0.39	0.2	0.59
M4	0.13	0.1	0.23
SD	0.13	0.1	0.23
Atmospheric	0.68		0.68
Sum			2.68
Measured			2.6 ± 0.4

Table IV: Calculated transmission losses of different transmission components for circular polarization under normal atmospheric pressure (140 GHz). The sum of the different contributions is compared to the measured total losses.

Figure captions

- Figure 1:** Schematic design of the 140 GHz/10 MW ECRH-plant for W7-X (cross section).
- Figure 2:** Front end of the beam tube with an absorbing layer of water cooled Teflon pipes (upper right side) wound to the inner surface. An additional absorbing structure, the so called ‘japanese umbrella’ is seen on the left side behind Mirror 1. The axes of symmetry of the directed high power beam is sketched in yellow, the stray radiation is sketched in blue.
- Figure 3:** MBWG section in the underground transmission duct. **Top:** Two retro reflectors are seen in the foreground, the two large stray- radiation absorbers are seen in the background. The bundle of 5 beams is transmitted through the central hole and the axis of the beam bundle is indicated. **Bottom:** Detail of the retro reflector, the axis of the incident and reflected beams are indicated in yellow, the axis of symmetry and the rotation direction is also shown.
- Figure 4:** Top: Relative losses in Polarizer P2 as a function of the rotation angle of polarizer P1. 0 deg corresponds to a linear, 45 deg to a circularly polarized wave, the incident beam power is 590 kW. Middle: Same for fixed angle of polarizer P1 at 0 deg (corresponding to linear polarization) as a function of the rotation angle of Polarizer P2 (0 deg corresponds to polarization parallel, 90 deg to polarization perpendicular to the corrugation grooves). Bottom: Absorbed power as a function of the incident wave beam power for fixed angle of P1 (45 deg, circular polarization) and P2 (20 deg).
- Figure 5:** Calorimetric measurement of the rf-power P_{refl} (after transmission through 10 mirrors) as a function of the incident rf-power P_{inc} . The dashed-dotted line indicates no-loss transmission.

Figure 1

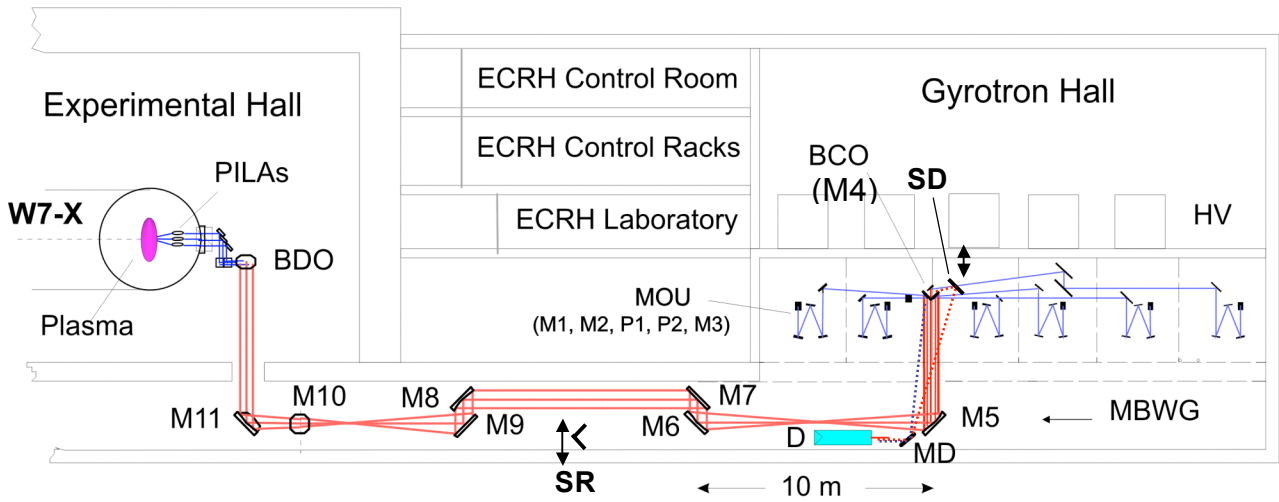


Figure 2

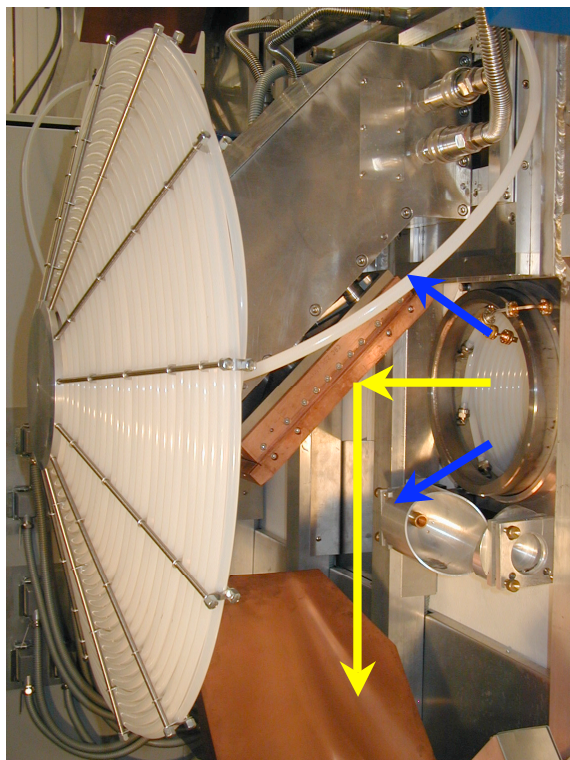


Figure 3

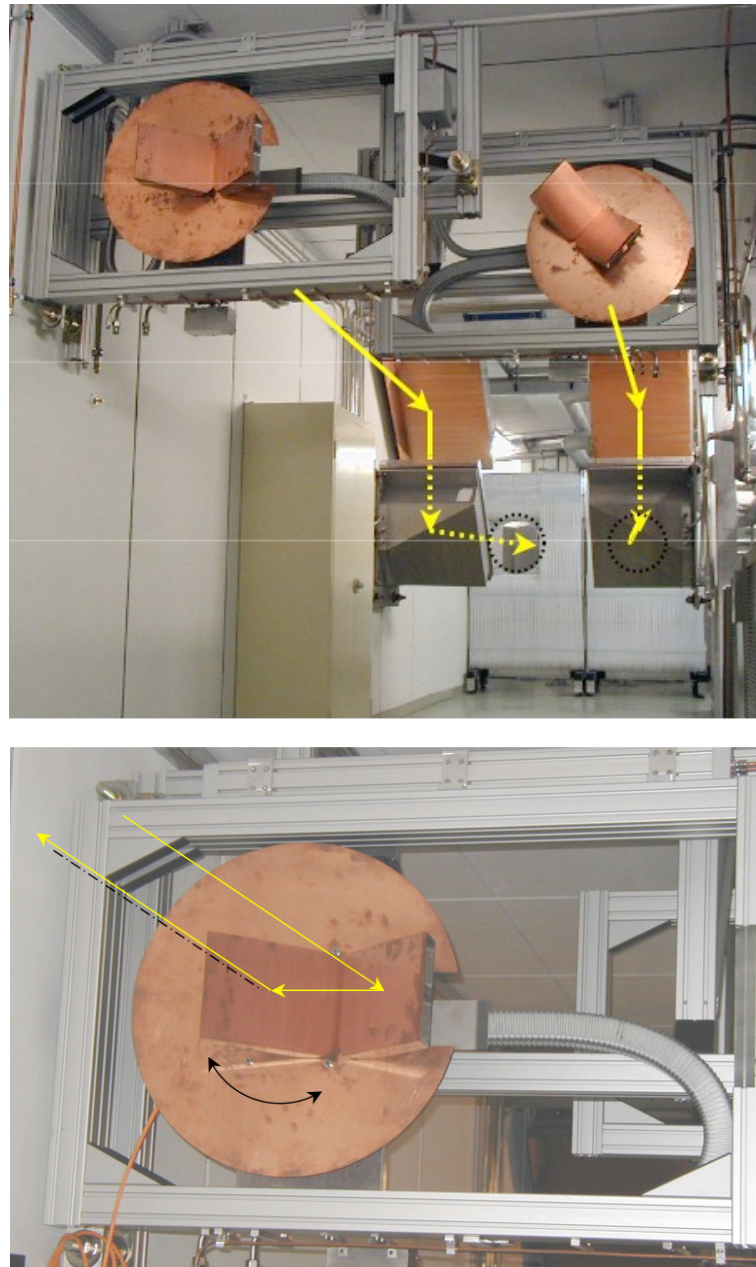


Figure 4

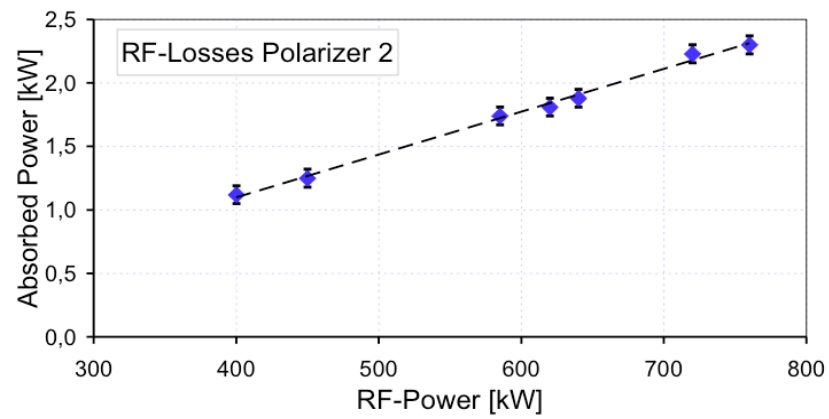
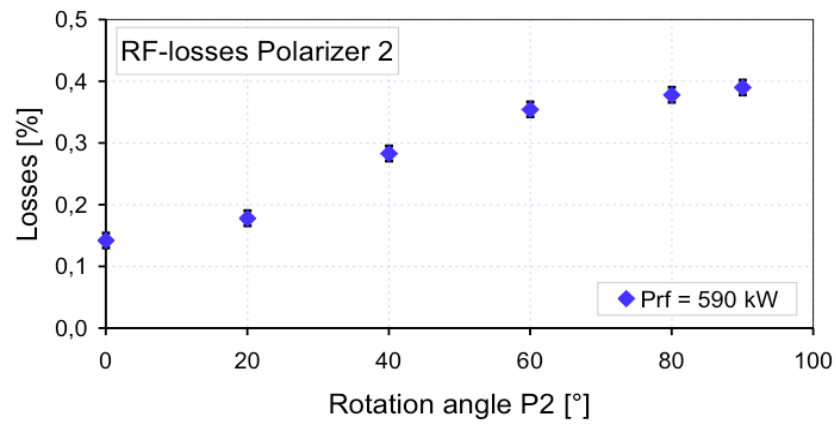
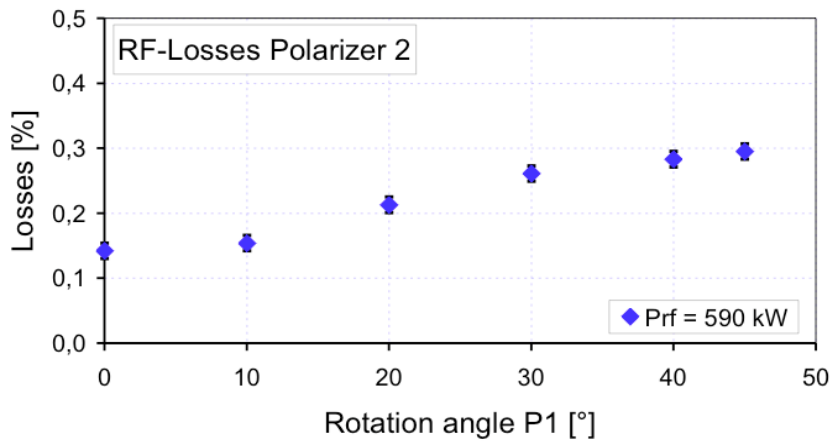


Figure 5

